

# An Array of *E*-Shaped Probe-Fed Microstrip Elements for Wireless Communications

Marcos V. T. Heckler, Eduardo S. Neves, Ricardo Schildberg, and J. C. da S. Lacava  
Instituto Tecnológico de Aeronáutica, São José dos Campos SP, Brazil

Lucio Cividanes  
Instituto Nacional de Pesquisas Espaciais, São José dos Campos SP, Brazil

**Abstract** — This paper discusses a new microstrip antenna array for wireless communication. Initially, the basic array element, an *E*-shaped probe-fed patch, is analyzed by comparisons between numerical and measured results. After that, a two-element subarray is discussed. Simulated results, obtained by using Ensemble 8.0™ and IE3D™ packages, and experimental ones are presented. Good agreement between these results is obtained. Finally, a six-element array is designed and analyzed by numerical computations.

## I. INTRODUCTION

In mobile communication systems, antennas are used to establish a radio link between radio stations when at least one of them is moving. In many cases, one is a mobile radio station while the other remains fixed [1]. This is the case of cellular phone systems, where some users (vehicles or people) carry portable handsets while radio base stations are the keys to establish the radio link. This is the main reason that makes a good design of the base station antennas essential. Therefore, considerations must be taken into account in order to minimize interference between two adjacent base stations and to reduce the transmitted power level necessary for a good signal communication with the mobile receivers.

In this paper, an array of six *E*-shaped elements is proposed to provide good radiation characteristics, mainly in terms of radiation pattern, in the entire American PCS, D and E Brazilian cellular communication bands.

## II. BASIC ARRAY ELEMENT

The element to be used to design the array is an *E*-shaped probe-fed microstrip element, which has been already reported in the literature [2,3]. In contrast with other wideband geometries, that usually have parasitic elements in the same layer [4] or stacked on the top of the main element [5], the *E*-shaped antenna presents a wider bandwidth with a single patch that are the antenna

M. V. T. Heckler, heckler@ele.ita.br, E. S. Neves, eneves@ele.ita.br, R. Schildberg, schild@ele.ita.br, J. C. da S. Lacava, lacava@ele.ita.br, Tel +55-12-3947-6811, Fax +55-12-3947-5878; L. Cividanes, lucio@dea.inpe.br, Tel. +55-12-3945-6232, Fax +55-12-3945-6225.

The authors would like to thank to Instituto de Pesquisas Eldorado – IPE and to Fundação de Amparo à Pesquisa do Estado de São Paulo – FAPESP, No. 01/00584-5, for the partial support of this work.

features desired in many wireless applications. *E*-shaped elements with 30 % of bandwidth have been recently reported [2].

In this paper, using the IE3D™ and Ensemble 8.0™ CAD tools, the *E*-shaped element was designed to operate with the central frequency at 1.9 GHz. The length and width of the slots and the position of the coaxial probe were determined to achieve a good impedance match in a wide bandwidth. The final dimensions of the element and the probe position are given in the Fig. 1.

The antenna was built in a two-layer substrate with an air layer of 15 mm thick, and a CuClad 250GX layer of 1.524 mm thick and dielectric constant of 2.55. The upper layer is supported by non-conductive posts not shown in Fig. 1 for simplicity.

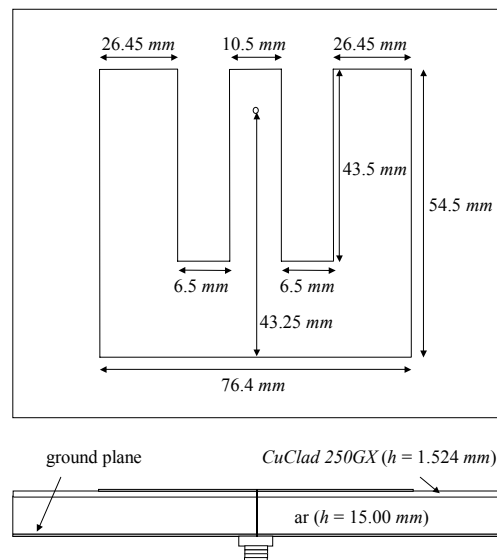


Fig. 1. Substrate layers for the *E*-shaped element.

Fig. 2 presents a comparison between computed values, given by Ensemble 8.0™, and experimental results for *V**SWR*. The computed and measured curves have the same behavior with a frequency displacement of about 35 MHz, but adjustments can be easily made to put the antenna in the desired frequency operation range. The experimental bandwidth is about 19 % considering a *V**SWR* at 1.5:1.

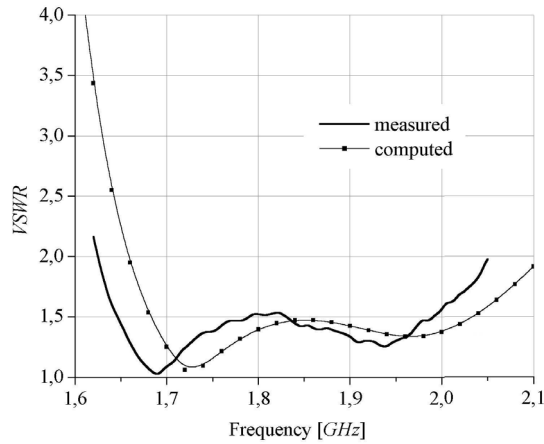


Fig. 2. Computed and measured results for the E-shaped antenna.

The radiation pattern was computed using *IE3D*<sup>TM</sup> software, considering a finite ground plane. Figs. 3 and 4 give the computed and measured radiation patterns in the E- and H-planes, respectively. In Fig. 3, only the co-polarization is shown because the cross-polarization level is 40 dB below the main lobe. From Fig. 3, one can observe that there is a good agreement between computed and measured radiation patterns. Also, the maximum radiation in the E-plane is about 11° displaced from the 0° reference point. Fig. 4 shows computed and measured co- and cross-polarizations. It can be observed that the maximum cross-polarization level in this plane is about 10 dB below the main lobe, which can be acceptable in many wireless applications [2]. There is also a good agreement between numerical and experimental results in this plane.

Before designing the array, numerical analyses of antenna sensibility with parameter changes were made. Variations of dielectric constant, mainly due to substrate tolerance, and changes in thickness of air substrate layer, caused by assembly errors, were studied. Changes in dielectric constant don't have great effect on the characteristics of the element because its thickness is thin compared with the air layer under the substrate (about 10%). On the other hand, changes in the thickness of air layer are critical, as shown in Fig. 5. Variations of 1 mm or more can significantly modify the VSWR curves.

### III. DEFINITIONS FOR THE ARRAY

It's necessary to define the desired features for the array before starting the design. Therefore, the specifications to be used are the same as those of a commercial antenna for the same application. The bandwidth is chosen to be between 1.7 GHz – 2.0 GHz, to comply with the D and E Brazilian cellular phone and American PCS bands. The lowest gain within the band is chosen to be 15 dBi and the maximum sidelobe level must be 10 dB below the principal lobe, so that uniform current distribution can be used to feed the array elements. The

geometry of the array is assumed to be linear, with elements uniformly spaced in order to provide a linear vertical polarization. The decision about the number of elements to satisfy the gain requirement was made by numerical computation of the gain for arrays of 4, 5 and 6 elements fed by currents of the same amplitude. The spacing between adjacent elements was chosen according

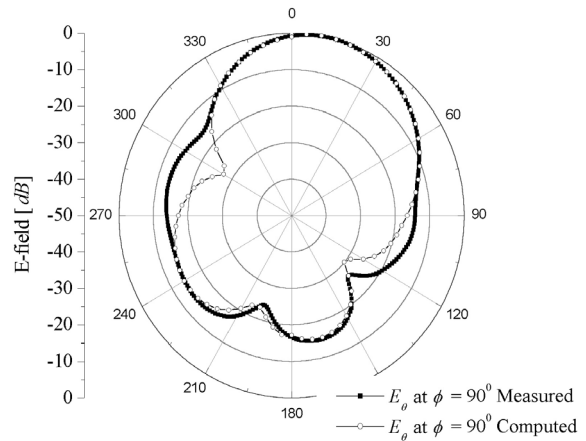


Fig. 3. Computed and measured radiation pattern in E-plane.

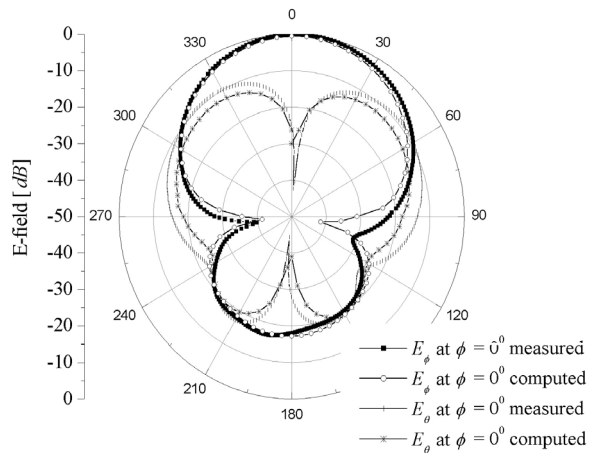


Fig. 4. Computed and measured radiation pattern in H-plane.

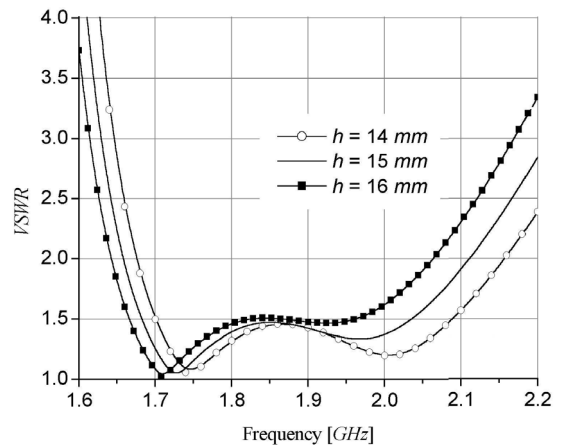


Fig. 5. Computed effect of thickness variations of the air layer.

to Fig. 6 [6], that represents the variation of the directivity of a broadside array of point sources versus the spacing between elements. The spacing in the three aforementioned cases was chosen to be in the maximum points of each curve so that the array directivity is maximized.

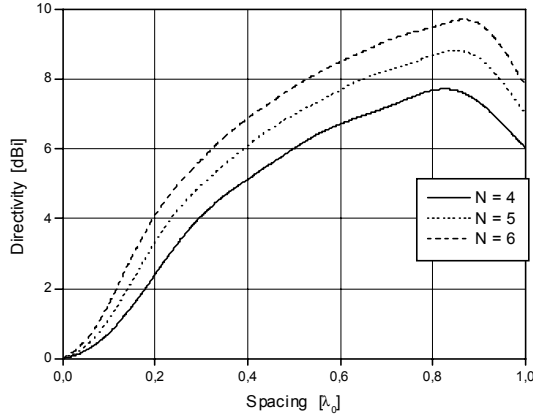


Fig. 6. Directivity (dB) versus spacing ( $\lambda_0$ ).

According to the curves shown in Fig. 6, the distance between elements for an array of 4, 5 and 6 elements are, respectively, 131 mm, 136 mm and 140 mm. Using the E-shaped element presented in section 2, the numerical results for the gain of arrays of 4, 5 and 6 elements are shown in Fig. 7. The curves indicate that the requirement of gain is just achieved with the array of 6 elements.

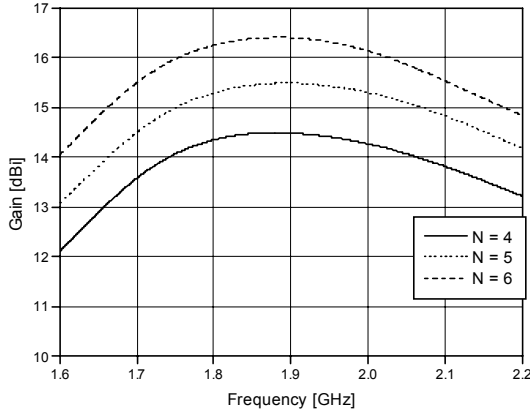


Fig. 7. Computed gains for the array of 4, 5 and 6 elements.

Therefore, the array must have 6 elements equally spaced due to the results presented in Fig. 7. A subarray of 2 elements was first studied and is described in the following section.

#### IV. TWO-ELEMENT SUBARRAY

A two-element subarray is studied in this section. The spacing between elements is kept the same as that of the 6-element array.

For some wireless applications, it's desired that the antenna system radiate a vertical linear polarized wave. Also, the beamwidth of the vertical plane (E-plane) may be narrower than that of the horizontal plane (H-plane). For these two reasons, the three possible array configurations are shown in Fig 8. For geometries 8.b and 8.c, there must be a phase shift of  $180^\circ$  between the two-excitation currents.

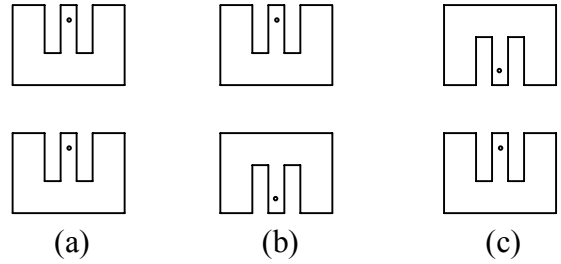


Fig. 8. Three possible geometries for the two-element subarray.

For these three arrays, computations were made considering spacing between elements of 140 mm, as depicted in section 3. For the three possible geometries, that one presented in Fig. 8.c is already analyzed in the literature [7] as an alternative to reduce the cross-pol level, as shown in Fig. 4. Using *IE3D<sup>TM</sup>* software, the gains for the three configurations were computed and are shown in Fig. 9. The computations were conducted considering finite ground plane of the same size (160 mm x 280 mm) in the three cases.

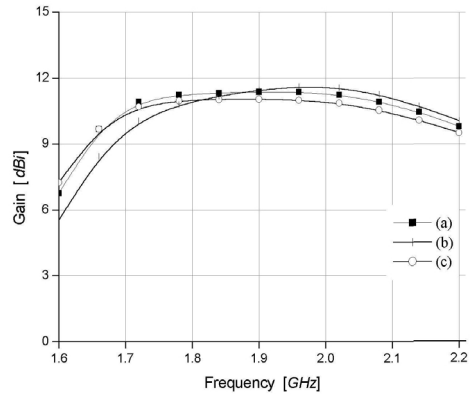


Fig. 9. Gain versus frequency for the subarrays of Fig. 8.

Fig. 9 shows that the geometry shown in Fig. 8.a presents the most constant gain along the desired band. It also presents the higher gain for frequencies below 1.9 GHz. In this frequency, the gain for geometries 8.a and 8.b is about 11.4 dBi and 11.0 dBi for the 8.c.

Fig. 10 shows the H-plane radiation patterns for the three geometries. Only the cross-polarization of geometry 8.a is shown because it's very low for the other two cases. The co-polarization in the H-plane pattern for the three cases is nearly the same and all of them are very

similar than that of a single element. On the other hand, the cross-polarization is still high for geometry 8.a.

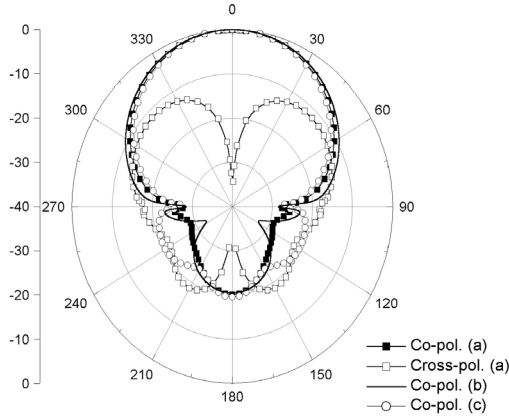


Fig. 10. H-plane radiation pattern for the three geometries.

Fig. 11 shows the E-plane for the three configurations shown in Fig. 8. Only principal polarizations are shown because cross-polarization levels are very small in all of the three cases. Fig. 11 clearly shows that 8.b and 8.c configurations present a symmetric E-plane radiation pattern. The displacement of the main lobe disappeared because there is a balance due to opposing orientation of the two elements.

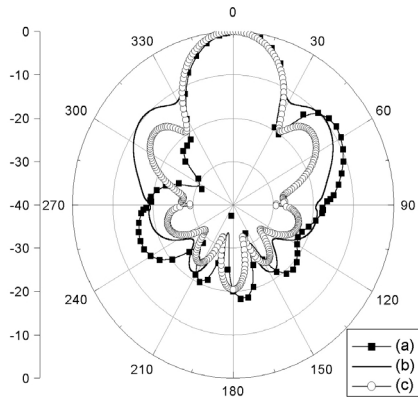


Fig. 11. E-plane radiation pattern for the three geometries.

The configuration shown in Fig. 8.a presents an asymmetric radiation pattern in E-plane due to the *E*-shaped element radiation pattern shown in Fig. 3. For base stations in land mobile communication systems, this feature may be desired because it reduces the frequency reuse distance [1], that can be a problem when more than one base station are nearly placed. This can also be improved by mechanically adjusting the tilt angle of the main beam of the array. Although this subarray presents this asymmetric pattern, its gain, as shown in Fig. 3, is approximately the same of those for the other two subarrays.

Due to aforementioned characteristics, a subarray similar than that of Fig. 8.a was designed, fabricated and measured. The feeder of the subarray is in the bottom side of the ground plane, as sketched in Fig. 12.

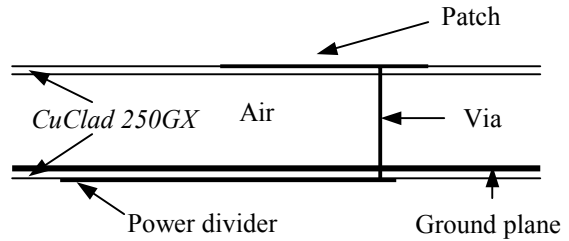


Fig. 12. Side view of the two-element subarray.

The feeder is a 1:1 power divider consisting in a T-junction and two  $\lambda/4$  transformers to achieve wide bandwidth considering *VSWR* at 1.5:1. The two elements are feeding by via as shown in Fig. 12. A photo of the subarray prototype is shown in Fig. 13.

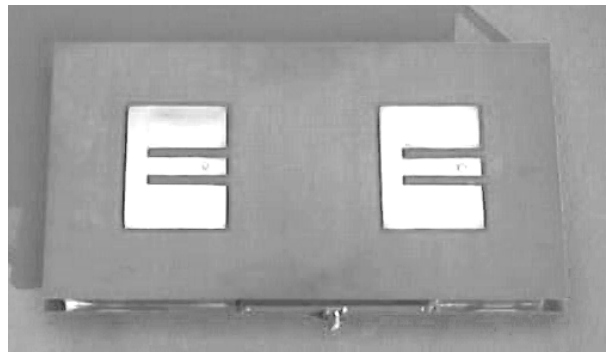


Fig. 13. A photo of the two-element subarray.

Figs. 14 and 15 show comparisons between measured and computed radiation patterns for the constructed subarray at 1.9 GHz. The computations were made using *IE3D*<sup>TM</sup> software, considering finite ground plane of the same size of that of the prototype. In the two planes shown, one can observe a good agreement between computed and measured results. As predicted by the simulations, the cross-polarization in the E-plane is very low. The backside radiation is about 20 dB below the maximum radiation level, so that it can be stated that it presents a good front-to back ratio.

## V. SIX-ELEMENT ARRAY

After analyzing the two-element subarray, it will now be considered the entire array of 6 *E*-shaped elements. In the previous sections, the numerical analyses were conducted considering finite ground plane. However, by hardware limitations, the simulation of the 6-element array will be performed considering infinite ground plane, because it reduces considerably the number of variables involved.

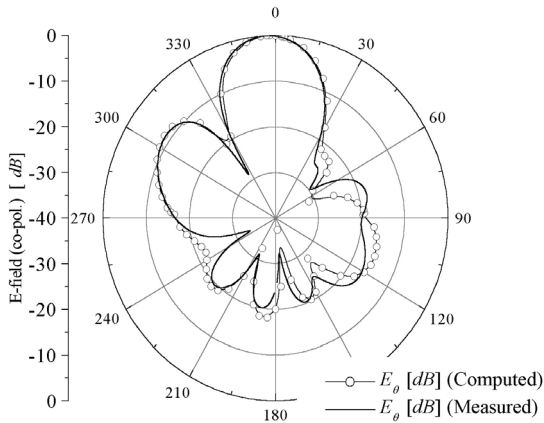


Fig. 14. E-plane radiation pattern for the subarray.

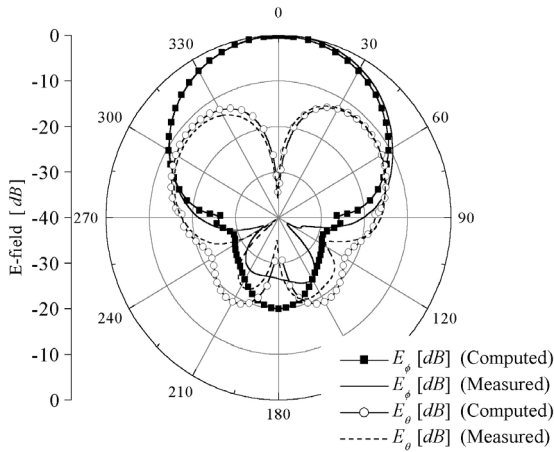


Fig. 15. H-plane radiation pattern for the subarray.

Once the power divider for a two-element subarray has already been developed, the next step is the design of a feeder in order to provide the same amount of power for the three subarrays. This is sketched in Fig. 16.

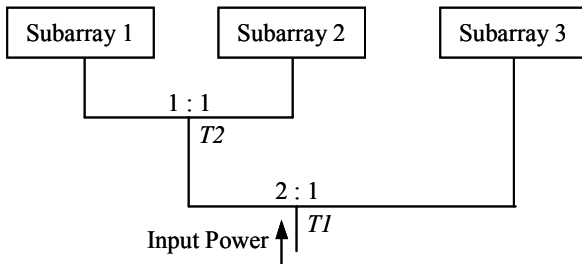


Fig. 16. Schematic illustration of the subarray power divider.

In  $T1$ , the resulting impedances of its two arms are  $75 \Omega$  and  $150 \Omega$ , so that a 2:1 power division ratio is achieved. In  $T2$ , the resulting impedances of Subarrays 1 and 2 have the same values, thus providing a 1:1 power division ratio. This power divider system makes the three subarrays be fed with powers of the same amount.

It's also desired to achieve the same electrical length

in the three paths in order to have a broadside radiation pattern. Using *Ensemble 8.0<sup>TM</sup>*, simulated curves for magnitude and phase of  $S$ -parameters were calculated and are shown in Figs. 16 and 17, respectively. In Fig. 17, the three output levels are  $-5.03 \text{ dB}$ ,  $-5.18 \text{ dB}$  and  $-5.17 \text{ dB}$  at  $1.9 \text{ GHz}$ . Considering that the ideal value for the magnitude of the  $S$ -parameters at the outputs should be  $-4.77 \text{ dB}$  and considering return loss negligible, the total power loss introduced by the feeder is  $7.6 \%$ . This is due to substrate loss tangent and the large length of the lines. The maximum variation between power levels at the outputs of the power divider is  $0.3 \text{ dB}$  what assures a balanced power division in the entire bandwidth. Also, as shown in Fig. 18, the three outputs present in phase signals in order to provide a broadside radiation by the array.

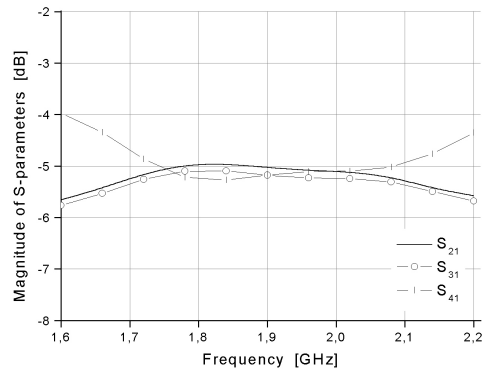


Fig. 17. Magnitude for  $S$ -parameters at the three feeder outputs.

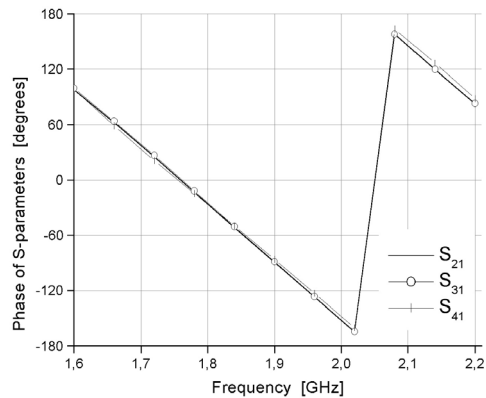


Fig. 18. Phase for  $S$ -parameters at the three feeder outputs.

Fig. 19 shows the computed  $VSWR$  curve with the outputs terminated with the six  $E$ -shaped elements. It is shown that the highest  $VSWR$  along the operation band is  $1.56$ , which is really close to the desired value.

Fig. 20 shows a comparison between *IE3D<sup>TM</sup>* and *Ensemble 8.0<sup>TM</sup>* packages on the computation of the E-plane radiation pattern. It can be seen that the result

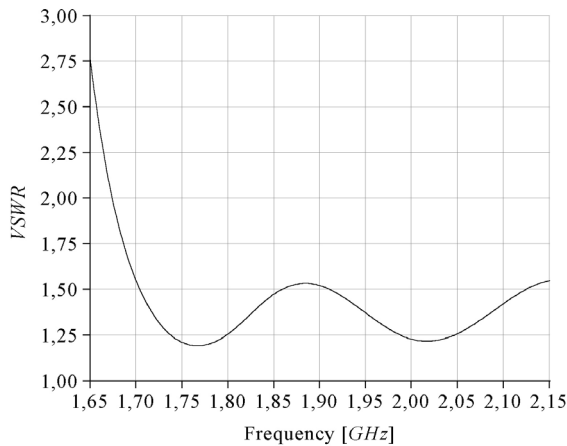


Fig. 19. Computed  $VSWR$  for the six-element array.

obtained by the former presents an asymmetric pattern, while that computed by the latter doesn't present this asymmetry. Once the element radiation pattern is asymmetric, the combined pattern must be asymmetric too. Then, comparing the results shown in Fig. 20, it seems that the radiation pattern prediction of  $IE3D^{TM}$  is more accurate for the present case.

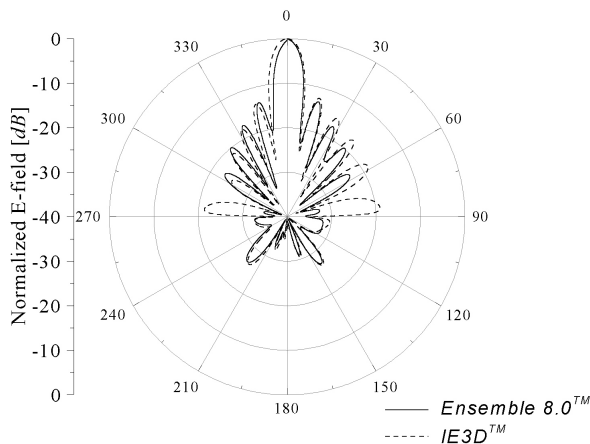


Fig. 20. Computed  $E$ -plane radiation patterns for the six-element array. For simplicity, only co-polarization is shown.

The low sidelobe level in one side of the main beam is still present in the radiation pattern of the six-element array, as it was in section 4. Also, the array provides a gain that allows the array to be installed in rural zones, where base stations are far from each other and high gain antennas are desired.

Because of the characteristics described above, the array is a potential radiator to be used in base stations for cellular phone applications.

## VI. CONCLUSIONS

The design and analysis of a six-element array was the main purpose of this paper. This array was designed to operate in the Brazilian cellular phone and American

PCS bands. Therefore,  $E$ -shaped elements were used because they have good performance in a wide bandwidth.

A two-element subarray was first designed and constructed. It was shown that computed and measured results are in good agreement, mainly in radiation pattern analysis. Three different configurations for the subarray were analyzed to choose the one that better fits the desired characteristics. The chosen configuration for the two-element subarray presents an asymmetric radiation pattern that can contribute to reduce the distance between two different base stations for mobile communications for frequency reuse purposes.

Finally, a six-element array was designed. Computations were performed using both  $Ensemble\ 8.0^{TM}$  and  $IE3D^{TM}$  to analyze feeder characteristics and radiation pattern of the resulting array. It was shown that the feeder outputs are all with equal amplitude and in-phase. Also, the desired asymmetric radiation pattern was also performed by the six-element array as it was by the two-element subarray. However, this feature is shown more effectively by  $IE3D^{TM}$ .

## REFERENCES

- [1] K. Fujimoto and J. R. James, *Mobile antenna systems handbook*, 2<sup>nd</sup> Ed., Artech House: Norwood, 2001.
- [2] F. Yang, X.-X. Zhang, X. Ye, and Y. Rahmat-Samii, "Wide-band  $E$ -shaped patch antennas for wireless communications", *IEEE Trans. Antennas Propagat.*, vol. AP-49, No. 7, pp. 1094-1100, Jul. 2001.
- [3] K.-L. Wong and W.-H. Hsu, "A Broad-band rectangular patch antenna with a pair of wide slits", *IEEE Trans. Antennas Propagat.*, vol. AP-49, No. 9, pp. 1345-1347, Sep. 2001.
- [4] G. Kumar and K. C. Gupta, "Directly coupled multiple resonator wide-band microstrip antenna", *IEEE Trans. Antennas Propagat.*, vol. AP-33, pp. 588-593, Jun. 1985.
- [5] D. M. Pozar, "Microstrip antenna coupled to a microstrip-line", *Electron. Lett.*, vol. 21, No. 2, pp. 49-50, Jan. 1985.
- [6] W. L. Stutzman and G. A. Thiele, *Antenna theory and design*, 2<sup>nd</sup> Ed., John Wiley & Sons: New York, 1998.
- [7] W.-H. Hsu and K.-L. Wong, "Broadband probe-fed patch antenna with reduced cross-polarisation radiation", in *Proc. 11<sup>th</sup> ICAP*, pp. 525-528, Apr. 2001.